JOURNAL OF THERMOPHYSICS AND HEAT TRANSFER
Vol. 8, No. 1, Jan.–March 1994

Influence of Injectant Mach Number and Temperature on Supersonic Film Cooling

K. A. Juhany,* M. L. Hunt,† and J. M. Sivo‡
California Institute of Technology, Pasadena, California 91125

The current work is an experimental investigation of the dependence of film cooling effectiveness on the injection Mach number, velocity, and mass flux. The freestream Mach number is 2.4, and the injection Mach numbers range from 1.2 to 2.2 for both air and helium injection. The adiabatic wall temperature is measured directly. The injection velocity and mass flux are varied by changing the total temperature and Mach number while maintaining matched pressure conditions between the injected flow and that of the freestream. The total temperature of the freestream is 295 K, and for the injection it ranges from 215–390 K. The results indicate an increase in film cooling effectiveness as the injection rate is increased. With the exception of heated helium runs, larger injection Mach numbers slightly increase the effective cooling length per mass injection rate. The results for helium injection indicate an increase in effectiveness as compared to that for air injection. Heated injection, with the injectant to freestream velocity ratios greater than 1, exhibit a rise in wall temperature downstream of the slot resulting in effectiveness values greater than 1. The experimental results are also compared with earlier studies in the literature.

Nomenclature

h_t = total enthalpy
M = Mach number
Re = Reynolds number
r = velocity ratio, u_i/u_∞
s = slot height
T_i = injection temperature
T_r = recovery temperature
T_t = total temperature
T_w = wall temperature
u_i = injection velocity
u_∞ = freestream velocity
X_{cl} = cooling length
x = streamwise distance
δ = boundary-layer thickness
η = film cooling effectiveness
λ = mass flux ratio, $\rho_i u_i/\rho_\infty u_\infty$
ν = kinematic viscosity
ρ = density

Introduction

NEW designs of supersonic and hypersonic vehicles have brought renewed interest in the areas of aerodynamic heating and active cooling techniques. One of the limiting design parameters for these vehicles is the maximum temperature and heat flux that is sustainable by the vehicle exterior and engine interior. For example, the afterburner temperature in an engine flying at Mach 5 is expected to exceed 2000 K.[1] An estimate of heating in the propulsion system is 10 kW/cm^2 with peak values upward of 50 kW/cm^2.[2] Although new materials and designs that integrate the propulsion system with the airframe are being introduced to account for the high temperatures and heat fluxes, the vehicles must also rely on active cooling techniques.

One proposed cooling method for supersonic or hypersonic flight is tangential slot injection or film cooling. Film cooling is a widely used technique to protect aircraft structures, rocket nozzles,[3] plug nozzles,[4] and turbine blades[5] from high-temperature environments. A thin layer or film of low-temperature gas is injected along the surface, in the direction parallel to the freestream. As the film-coolant fluid mixes with the higher temperature mainstream, the temperature of the gas film increases, reducing the film-cooling effectiveness. Previous experimental studies on film cooling have been predominantly in the area of incompressible flow. In the area of compressible flow, extensive work on film cooling has been done in cooling jet engine turbine blades. These studies involve flows with velocities below sonic conditions. Few studies have examined supersonic film cooling, especially with variable Mach number injection. More data are needed with low molecular weight gas injection as would be applicable to the National Aero-Space Plane. Furthermore, the results from existing supersonic film cooling studies vary considerably and little work has been done to resolve the discrepancies or to explain the physical phenomenon that impacts the mixing between the freestream and the injectant.[2]

The film-cooling flowfield can be divided into three regions[6]: 1) an inviscid core region, 2) a wall jet region, and 3) a boundary-layer region. The inviscid core region, like a free jet, contains a viscous layer that emanates from the lip and ends when it meets the growing slot-flow boundary layer. In this region the wall temperature remains constant at the recovery value of the injectant flow. The wall jet region starts at the location where the viscous layer originating from the lip meets the slot flow boundary layer. In this region, the wall begins to be affected by the mixing between the freestream and injectant. Due to intense mixing in this region, the temperature starts approaching that of the freestream value. Further downstream, the wall jet flow relaxes to a boundary-layer flow. Thus, film cooling flow combines different types of familiar flows: a free-jet flow, a wake flow, a shear layer flow, and a boundary-layer flow. Consequently, the behavior of the wall temperature should exhibit differences in each region.

Received Jan. 21, 1993; revision received June 7, 1993; accepted for publication June 8, 1993.

*Research Assistant, Department of Aeronautics. Student Member AIAA.
†Assistant Professor, Department of Mechanical Engineering. Member AIAA.
‡Research Assistant, Department of Mechanical Engineering. Student Member AIAA.

Table 1 Supersonic film cooling studies

Author	Fluid	M_∞	M_i	r	λ	P_i/P_∞
Goldstein et al.[11]	Air	3	≤1	≤0.5	0.1–0.41	≤1 and ≥1
	He	3	<1		0.01–0.02	<1
Cary and Hefner[12,13]	Air	6	1	0.29–0.35	0.03–1.6	≤1 and ≥1
Rouser and Ewen[14]	H_2	2.3	1.9	1.95	0.15–0.58	0.5–2.0
	N_2	2.3	1.9	0.54	0.47–2.2	0.5–2.0
Current	Air	2.44	1.2–1.9	0.57–1.1	0.38–0.77	1
	He	2.44	1.3–2.2	1.6–2.6	0.18–0.44	1

In incompressible flow, the film-cooling effectiveness is defined as

$$\eta = \frac{T_w - T_\infty}{T_i - T_\infty} \tag{1}$$

where T_∞ is the freestream temperature. An effectiveness of one corresponds with a wall that remains at the injection temperature, and the axial distance over which this occurs is referred to as the effective X_{cl}. The fluid is heated as a result of mixing with the main flow, and the effectiveness decreases with downstream distance.

Early work on film cooling[7] has shown that under certain conditions the value of the heat transfer coefficient with film cooling quickly approaches that of the undisturbed boundary-layer flow. The same conclusion can be obtained theoretically if the incompressible, constant property, energy equation is applied to the film cooling flow.[7] As a consequence, the value of the adiabatic wall temperature in Eq. (1) is often not obtained directly, but instead determined from measurements of the wall heat flux and from calculations of the boundary-layer heat transfer coefficient.

Film cooling in low-speed flows has been thoroughly investigated (as reviewed by Goldstein[8]). A common purpose of these investigations was to develop a correlation for effectiveness, as defined in Eq. (1). The effectiveness results are often plotted as a function of downstream x, divided by s, and by the ratio of coolant mass flux to that of the freestream λ, $x/(s\lambda)$ where $\lambda = \rho_i u_i/\rho_\infty u_\infty$. The dependence of η on $x/(s\lambda)$ is developed from integral models for air injection into an airstream.[8] The effect of foreign gas injection is incorporated in the integral analysis by including the specific heat ratios, and is usually presented as $x/(s\lambda)(c_{p\infty}/c_{pi})$.

For supersonic flow, the effectiveness is often defined by replacing the freestream temperature with the freestream recovery temperature $T_{r\infty}$

$$\eta = \frac{T_{rw} - T_{r\infty}}{T_{ri} - T_{r\infty}} \tag{2}$$

where T_{rw} and T_{ri} are the recovery temperatures measured along the surface and the recovery temperature of the injected fluid under adiabatic conditions. To correlate the data in high-speed flow, previous studies attempted to use modified incompressible flow correlations.[8] However, these correlations were not successful in predicting experimental measurements. The extension of the incompressible results to supersonic flow is complicated by two issues that are characteristic of high-speed flows: 1) the strong coupling between the momentum and energy equation, and 2) the appearance of shock waves. As a consequence of the strong coupling between the momentum and energy equations, the thermal features of the flow are strongly influenced by the hydrodynamic aspects. Unlike incompressible flow, the heat transfer coefficient with injection is expected to be different than the value of the undisturbed boundary layer. Beckwith and Bushnell[9] and Banken et al.[10] showed that the heat transfer coefficient with injection can differ significantly from that without injection. Therefore, the adiabatic wall temperature in Eq. (2) should be determined directly and not be inferred from the heat flux.

Studies of film cooling in which the adiabatic wall temperatures were measured directly, include the works of Goldstein et al.,[11] Cary and Hefner,[12,13] Rousar and Ewen,[14] and Baryshev et al.[15] The work by Goldstein et al.[11] considered sonic and subsonic injection of air and helium into a Mach 3 freestream. Both the injectant and the freestream flows were laminar, and the boundary-layer thickness at the injection slot was smaller than the slot height of the injectant (δ/s from 0.18 to 0.4). Goldstein et al. defined their effectiveness by replacing $T_{r\infty}$ in Eq. (2) with the recovery temperature measured with the injection of fluid at the same total temperature as the freestream. The results demonstrated that sonic injection of air significantly increased the film cooling effectiveness over that for subsonic injection.[11] In addition, the helium results indicated that the higher heat capacity of the injected fluid further increased the effectiveness. However, the helium studies were only performed for subsonic injection Mach numbers. Table 1 summarizes the parameters for this study and for other comparable studies.

The work by Cary and Hefner[12,13] involved sonic air injection into the hypersonic flow at Mach 6, and the results showed further increases in effectiveness over the supersonic results by Goldstein et al. In these experiments the freestream flow was turbulent and the boundary-layer thickness at the injection nozzle was considerably larger than the slot height (δ/s from 4.6 to 32). Cary and Hefner's definition of effectiveness was based on the freestream stagnation temperature $T_{t\infty}$ instead of $T_{r\infty}$ defined in Eq. (2). The results indicated that the effectiveness increased with injection temperature.

Rousar and Ewen[14] injected both hydrogen and nitrogen at Mach 1.9 into an airflow at Mach 2.3. The boundary layer was turbulent, but its thickness was not given. The effective cooling lengths for air injection were less than those found in the studies by Goldstein et al.[11] and by Cary and Hefner,[12,13] which could be due to differences in the experimental conditions. For hydrogen injection, the effective cooling lengths were larger than for any of the air studies, and the decrease in effectiveness as a function of downstream distance was significantly less for hydrogen. The injection Mach number and temperature remained constant, while the mass flow rates were varied by changing the injection pressure, so that the injectant was either underexpanded, overexpanded, or at matched conditions. The resulting mass flux ratios were $0.15 < \lambda < 0.58$ for hydrogen, and $0.47 < \lambda < 2.2$ for air.

To compare the air and hydrogen results, Rousar and Ewen modified the effectiveness definition using the difference in enthalpies

$$\eta = \frac{h_{t\infty} - h_{tw}}{h_{t\infty} - h_{ti}} \tag{3}$$

where $h_{t\infty}$ indicates the total enthalpy of the freestream and h_{tw} is the total enthalpy for the edge of the viscous sublayer for adiabatic conditions. This definition is useful in presenting results for dissimilar gas injections; however, the definition relies on models for the entrainment rate to determine h_{tw}.

In addition to these studies, several film-cooling studies have measured the wall heat flux by using the transient techniques.[16–21] The studies by Alzner and Zakkay,[16] Zakkay et al.,[17] and Parathasarathy et al.[18] used a transient thin wall technique, where the heat transfer is determined from the

rate of change of the surface temperatures. The heat transfer coefficient value was calculated using flat plate turbulent boundary-layer correlations for flow without injection. As indicated earlier, this indirect method of determining the adiabatic wall temperature and the film cooling effectiveness can lead to significant errors because the heat transfer coefficient with injection can differ significantly from values without fluid injection.

In recent hypersonic film-cooling effectiveness studies[19-21] the heat transfer was measured using thin film resistance thermometers in a shock tunnel. The surface heat flux was measured with and without fluid injection. The no-injection boundary-layer results were used to determine the heat transfer coefficient. These boundary-layer heat transfer coefficients were then used with results of the injection experiments to calculate the film cooling effectiveness. Although, the measurement of heat flux was direct, and therefore more accurate than the studies of Refs. 16–18, obtaining the adiabatic wall temperature with injection by using the heat transfer coefficient without injection results in inaccuracies.

The approach in this experiment is to obtain the adiabatic wall temperature directly by insulating the wall. The data are compared to studies of Goldstein et al.,[11] Cary and Hefner,[12,13] and Rousar and Ewen[14] in which the adiabatic wall temperatures were measured directly.

Experimental Facility

In the current experiment, air and helium were used as the injectants, and the injection Mach number varied from M_i = 1.2 to M_i = 2.2. The mass flow rates were varied by controlling the injection temperature, injection Mach number, and matching the injection exit pressure to that of the freestream. The ranges of parameters for the present experiments are listed in Table 2.

The experiments were conducted in the Graduate Aeronautical Laboratory, California Institute of Technology (GALCIT) continuous supersonic wind tunnel. Figure 1 shows a schematic of half-nozzle configuration used in the slot injection experiments. Air entered the wind tunnel at ambient

Table 2 Experimental parameters

Injectant	$T_{ti}/T_{t\infty}$	M_i	U_i/U_∞	$\rho_i U_i/\rho_\infty U_\infty$
Air	1.13	1.3	0.72	0.38
	1.13	1.5	0.82	0.50
	1.13	1.8	0.91	0.61
	1.14	2.2	1.0	0.82
	1.32	2.2	1.1	0.77
	0.80	1.2	0.57	0.40
	0.76	1.5	0.66	0.59
	0.76	1.8	0.73	0.74
Helium	1.16	1.3	2.0	0.18
	1.16	1.6	2.2	0.23
	1.16	1.9	2.4	0.30
	1.24	2.2	2.6	0.34
	0.75	1.3	1.6	0.20
	0.71	1.9	1.9	0.44

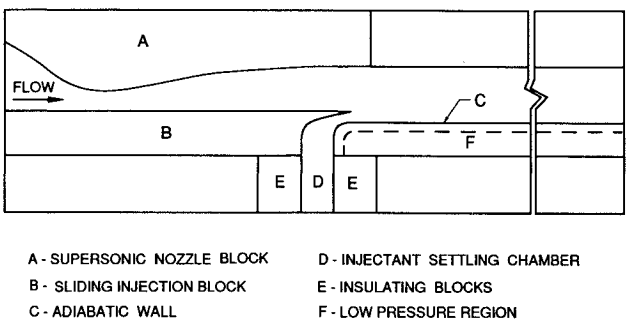

Fig. 1 Schematic of wind-tunnel test section. Drawing not to scale.

pressure (≈0.97 atm) and temperature (≈28°C). At the beginning of the test rhombus where the injectant slot was located, the boundary layer was turbulent with a thickness of 3.4 mm and a *Re*/m of 9.0 × 10^6. The nominal freestream Mach number was 2.44 ± 0.02. The total test section length and height were 400 and 25.4 mm, and the slot height at the exit of the injection nozzle was 1.5 mm.

The 2-mm-thick instrumented plate was made from Hastelloy-X®, a low thermal conductivity nickel-cobol alloy used to reduce conduction from the injection slot to the downstream section and from the plate sides. To minimize heat transfer from the instrumented plate to the exterior, the region behind the plate was open to the low-pressure downstream environment. Fifty-nine thermocouples were mounted on the back side of the plate. The thermocouples were epoxied into 1-mm holes, laser-drilled 0.3 mm below the surface. The plate also contained 48 pressure taps of which only 25 were connected for this experiment. The pressure taps were connected to piezoelectric transducers. The thermocouples and pressure taps were arranged in a diagonal fashion in the central third of the plate to provide concentrated measurements of pressure and temperature without interference. The diagonal arrangement made it possible to assess any heat exchange through the sides of the plate to the environment. All thermocouples and pressure transducers were connected to a PC-based data acquisition system. The wind tunnel was also equipped with a combined continuous and 10-ns spark source schlieren system for flow visualization.

The injectant gas was supplied from compressed gas bottles that were connected to a manifold and a pressure regulator. The regulator was used to adjust the pressure of the injectant before entering the turbine flow meter. Using the flow meter, the uncertainty in the mass flow measurements was approximately 5%, with the largest values occurring at the highest flow rates. After metering the flow, the injectant entered a heat exchanger that was used to increase or decrease the injectant temperature. For heated runs, the total temperature was increased to approximately 70°C using resistance tape heaters that were controlled with a variable voltage regulator. A few tests were made at a higher temperature (<120°C) to indicate the effect of further heating. Additional heating of the injectant would have resulted in an unfavorable heat conduction to the freestream boundary layer through the injectant-nozzle lip. For cooled runs, a dry-ice/alcohol mixture was used to decrease the injectant temperature to approximately −60°C. After exiting the heat exchanger, the flow was throttled to the injection reservoir where the total and static pressures, and the total temperature were measured. The total pressure was measured using a tube that faced the direction of the flow while the static pressure was measured at the wall; the difference between the two measurements were small, indicating that the flow was stagnant. To reduce conduction upstream to the primary flow, the injection reservoir was made from a wooden block.

Figure 2 shows the sliding block injection nozzle. The end of the sliding block was tapered to an angle of 10 deg which was used to form the injection nozzle. The lip thickness in this study was difficult to define since the lip had a wedge shape with a sharp trailing edge (0.25-mm thick). By moving the sliding block, the Mach number was varied by changing the height of nozzle throat. The termination of the nozzle at 10 deg resulted in a radial-type flow, similar to that of rocket nozzles, so that the flow out of the nozzle was not parallel to

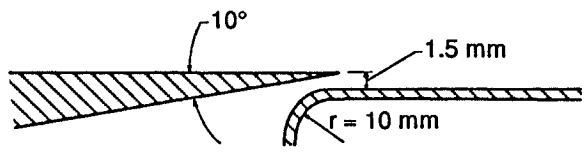

Fig. 2 Injection nozzle geometry.

the freestream flow. The effect of the injectant radial flow on the flow just downstream of the nozzle is discussed in the next section.

The injection Mach number reported in the study was determined from the height of the nozzle exit (1.5 mm) assuming zero displacement thickness, and by measuring the total temperature, total pressure, and mass flow rate of the injected gas. This method of calculating the Mach number agreed with the Mach number measured with the pitot probe at the center of the slot exit ($M \pm 0.1$) for Mach numbers 1.5 and higher.[22] However, the accuracy for the transonic Mach number injections range (≤ 1.2) was within $M \pm 0.2$, with Mach numbers always greater than unity. The calculation assumed a zero displacement thickness through the nozzle. The agreement between the calculation method and the pitot probe measurement indicated that the displacement thickness was small. A static pressure tap was also located within the nozzle, and this tap was used to verify that the flow within the nozzle was supersonic. The pressure tap located nearest to the slot was also checked to verify that the pressure was near matched conditions.

Experimental Results

Preliminary experiments were made to assess the effect of heat conduction between the environment and the test section, and to examine the impact of the backward facing step formed by the slot and the instrumented plate. As indicated by the thermocouples located nearer to the side walls of the test section, some heat conduction occurred along the edge of the plate. Without fluid injection, the adiabatic wall temperatures were at most 8°C higher than the value predicted assuming a turbulent recovery factor of 0.89 and using the total temperature of the freestream. The variation of the wall temperature from the expected adiabatic wall temperature without injection resulted from several factors: the upstream history effect on the boundary layer, the impingement of the step shock wave on the plate, and conduction. As observed in the schlieren system and through the static pressure taps, this shock was reflected several times within the test section. The temperatures measured near the sidewall of the tunnel were close to the temperature located at the center of the plate (less than 1°C), indicating low conduction along the sides of the plate. The plate responded quickly to temperature variations, but the wind-tunnel glass windows and the wooden injectant reservoir slowly reached thermal equilibrium. In all runs, sufficient time was given for the plate and the injectant reservoir to reach thermal equilibrium, usually 15 min. Correcting the effectiveness for conduction proved to be difficult because the heat transfer coefficient with injection is unknown.

The flow parameters for the 10 different experiments are listed in Table 2. The air experiments are for Mach numbers between 1.2–2.2, mass flux ratios between $0.38 \leq \lambda \leq 0.82$, and velocity ratios between $0.57 \leq r \leq 1.1$. The helium experiments are for Mach numbers from 1.2 to 2.2, mass flux ratios between $0.2 \leq \lambda \leq 0.44$, and velocity ratios between $1.6 \leq r \leq 2.6$. The definition of effectiveness for the presentation of the experimental results corresponds to the definition in Eq. (2), where $T_{r\infty}$ is the measured adiabatic wall temperature without fluid injection. The value of T_{ri} is the wall temperature measured just downstream of the injection nozzle. Using the measured values of $T_{r\infty}$ and T_{ri}, rather than the calculated values, gives a more accurate value of effectiveness.

Flow visualization studies using the schlieren optics were undertaken to investigate the flow downstream of the slot. The nozzle was set to an injectant Mach number, then the injection mass flow rate was increased until its value reached the matched pressure condition. As the injectant flow rate was increased towards the matched pressure value, a similar shock structure to the studies of Goldstein et al.[11] was observed. Figure 3 is a schlieren photograph of a Mach 2.2 slot flow, which is a typical flow pattern for all the other injectant Mach numbers. The knife edge for the schlieren photograph is positioned parallel to the flow direction. The schlieren photograph shows the freestream boundary layer interacting with the injectant. The injectant is the bright region next to the wall, while the freestream boundary layer is the dark region just above the injectant. The injectant at the point of interaction is at an angle of 10 deg, with respect to the parallel free-stream. Although the injectant and the freestream are at matched pressure, a shock wave in both the freestream and injectant sides is produced to adjust the flow to the same orientation angle. The slot flow radial velocity is reduced as the wall is approached on the injectant side. The interaction between the freestream and the injectant flow starts at the slot tip. The disturbance due to the interaction is propagated through the Mach lines. The streamlines closer to the wall feel the disturbance at a larger axial distance from the slot exit than streamlines farther from the wall. Consequently, the streamlines closer to the wall expand more than ones farther away from the wall, increasing in Mach number and decreasing in pressure. Therefore, the shock wave, produced in the injectant flow, increases in strength as it approaches the wall. The injectant shock wave interacts with the laminar boundary layer, resulting in separation, but reattachment soon follows because the boundary layer is small and the strength of the shock wave appears to be close to the incipient value. The above information concerning the shock structure out of the slot was examined computationally,[23] using the MUSCL scheme developed by Lappas.[24] It was found that the shock wave strength in the injectant flow, measured in terms of static pressure rise, ranged from 1.1 to 1.3 for the lowest and highest injection Mach number, respectively. The leading separation shock, the expansion wave, and the recompression shock (characteristic of shock wave boundary-layer separation) are indicated by two sharp bright lines surrounding a dark region (expansion wave). The effect of weak shock waves on the adiabatic wall temperature is not significant,[22] especially next to the slot. Previous results[17] indicate that the slot-flow lip shock wave does not seriously degrade film cooling effectiveness.

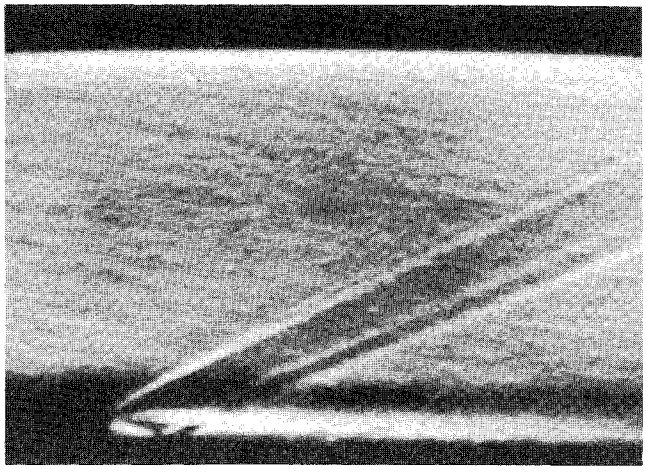

Fig. 3 Schlieren photograph of $M_i = 2.2$ air injection.

The addition of mass by injection in the fixed test section area resulted in a pressure increase that was proportional to the injection rate. Figure 4 shows a selection of wall pressure distributions for some of the tests. The pressure distribution along the wall indicates that the pressures for most runs are nearly constant for the first 60 slot heights, but gradually the pressure begins to increase. The highest pressure increase is from 6.2 kPa near the injection slot to 9.6 kPa at $X/s = 300$ for the $\lambda = 0.74$ case. The spikes in the pressure profile are a result of the lip shocks propagating through the test section and impinging on the wall. Although the shock waves in the tunnel are weak, their signature on the wall indicates the

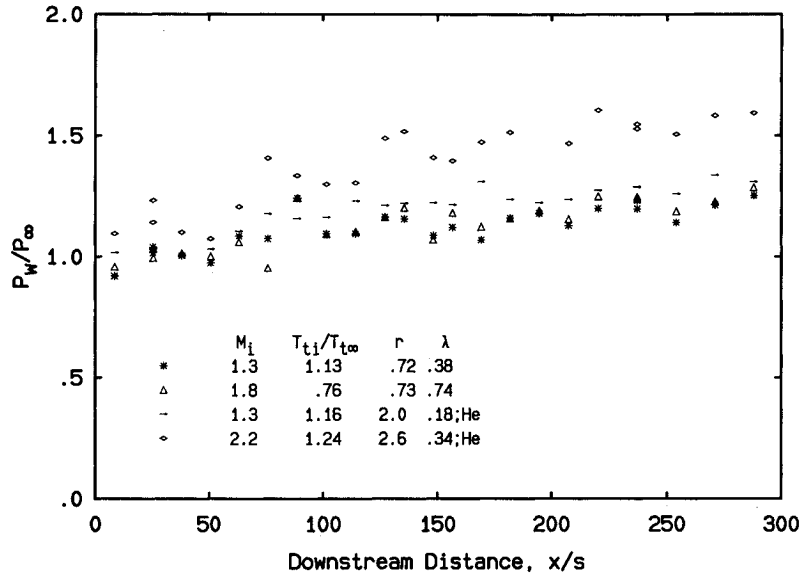

Fig. 4 Wall static pressure distribution for air and helium injection.

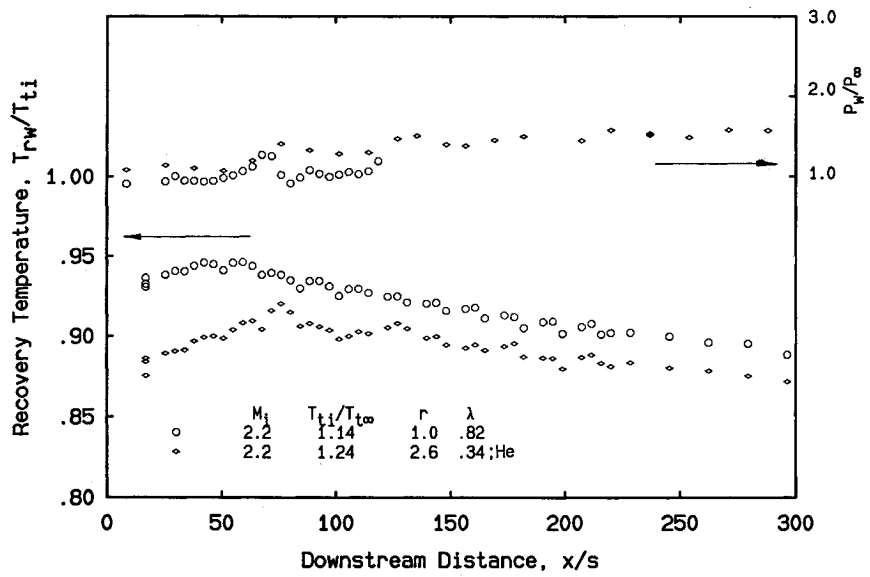

Fig. 5 Temperature and pressure ratios of heated helium and air injections displaying an increase in temperature downstream of the slot. The upper data set are the pressure ratio, while the lower ones are the temperature ratio.

added effect of the reflected shock. In previous low-speed film cooling experiments, it was found that pressure gradients of the magnitude experienced under the current experimental conditions did not influence the film cooling effectiveness,[8] while the effect of pressure gradient in supersonic flow (not associated with shock waves) is not well documented. The comparisons in this study are based on the assumption that the pressure gradients of the magnitude experienced in the current experiments have little effect on the film cooling effectiveness.

As discussed earlier, a typical plot of temperature with heated injection vs distance downstream of the slot shows the temperature near the slot to be constant for a short distance in the inviscid core region. Then the temperature drops as the freestream mixes with the injectant. The opposite trend occurs when a cold injectant is used. In general, for both heated and cooled injection, the effectiveness value follows the same temperature trend. However, for heated injection at high velocities ($r \geq 1$), there is a distance downstream of the slot where the recovery temperature increases at constant pressure, even beyond the temperature T_{ri}. This increase in temperature results in an increase in effectiveness with downstream distance to values above 1, as defined by Eq. (2). This phenomenon is demonstrated in Fig. 5, which shows results of temperature normalized by the injectant stagnation temperature, and pressure normalized by the freestream pressure for Mach 2.2 heated injection of air and helium. The length in which this rise occurs is shown to extend to 45 slot heights in the case of air, and 70 slot heights in the case of helium. The increase in temperature is a result of the flow near the wall, composed of mostly injectant fluid, slowing down due to the mixing process between the freestream and the injectant.[22] Additional heating would also occur when the injectant boundary layer transitions from a laminar to a turbulent boundary layer. This rise in temperature should also occur with cold injection, but the effect is not noticeable since the temperature also rises due to the mixing with the hotter freestream.

Figures 6–9 show the film cooling effectiveness as a function of downstream distance divided by slot height x/s. Data above $\eta > 1$ is not shown, but it occurs for all heated injection whose r is greater than 1. The highest effectiveness values obtained in the cases of data sets shown in Fig. 5 are 1.2 and 1.5 for air and helium injection, respectively. As indicated in the figures, X_{cl} ranges from approximately 30 to 300 slot heights depending on the fluid, the injection rate, and the Mach num-

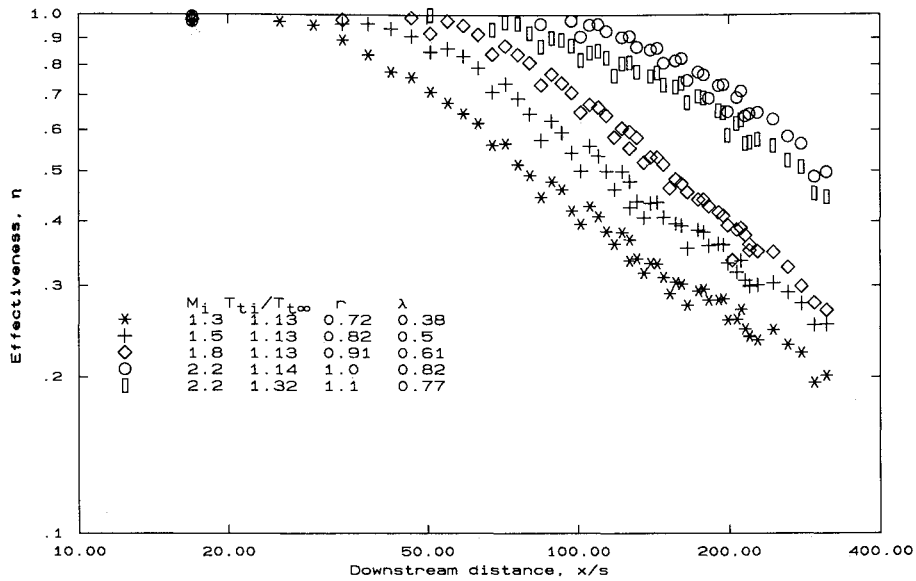

Fig. 6 Heated air injection, η as a function of x/s.

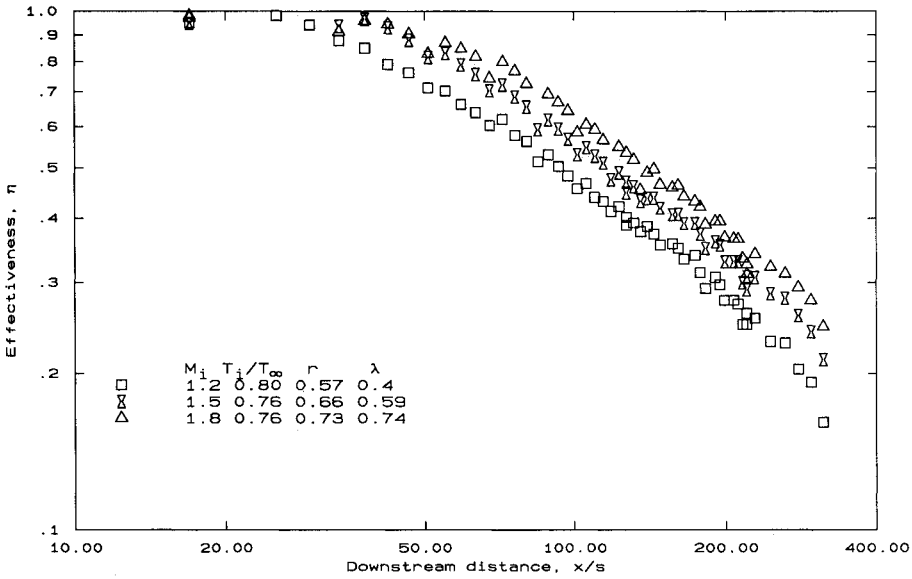

Fig. 7 Cooled air injection, η as a function of x/s.

ber. The decrease in effectiveness downstream of X_{cl} also appears to depend on these parameters.

In Fig. 6 the results are presented for heated air injection ($T_t \approx 70$°C). For a fixed injectant temperature, increasing the injectant Mach number raises both the velocity ratio and mass flux ratio which results in an increased cooling length. By comparing the results for $M_i = 1.3$ and $M_i = 1.8$, the increase in cooling length is approximately $30s$, but requires a 60% increase in mass flux. When increasing the injection Mach number to 2.2, corresponding to a velocity ratio of unity, the rate of decay of effectiveness is reduced compared to other Mach number injections. Additional heating of the Mach 2.2 injection to a value of $T_{ti}/T_{t\infty} = 1.32$ results in a 10% increase in velocity and a 6% reduction in mass flow rate, but only results in a small change in effectiveness. Figure 7 shows results for cooled air injection ($T_t \approx -40$°C). For cooled injection, the results for $M_i = 1.8$ indicates only a slight increase in cooling length beyond the results for $M_i = 1.5$. When the Mach number is increased to 1.8 in both cases of heated and cooled injections, the improvement in effectiveness is less in the case of cooled injection, whose increase in λ is even higher than that for the heated injection.

Figure 8 shows the results of effectiveness with heated helium injection. The results show a large change in effectiveness when the injection Mach number is increased from 1.3 to 1.6. High effectiveness values (greater than 0.8) are achieved for the entire test length of 300 slot heights, when the injection Mach number is more than 1.6. Figure 8 also shows that effectiveness does not improve beyond the Mach 1.9 value, corresponding to a velocity ratio of $r = 2.4$. The injectant of Mach 2.2 is at a higher temperature and produces similar effectiveness values to the Mach 1.9 case. Figure 9 presents the measurements for the cooled helium injection studies. The results show an increase in cooling length of approximately $20s$ for a 120% increase in the fluid injection rate. The cooled helium injection produces cooling lengths much smaller than that produced by the heated helium injection. In contrast to air injection, increasing the helium velocity ratio beyond 1, $r > 1$, increases the effectiveness until the value of $r = 2.4$ is reached.

Figure 10 presents the effectiveness results for all of the experimental runs as a function of $x/(s\lambda)(c_{p\infty}/c_{pi})$, which is the parameter suggested by the integral analyses.[8] As shown in the figure, the parameter $x/(s\lambda)(c_{p\infty}/c_{pi})$ nearly collapses all

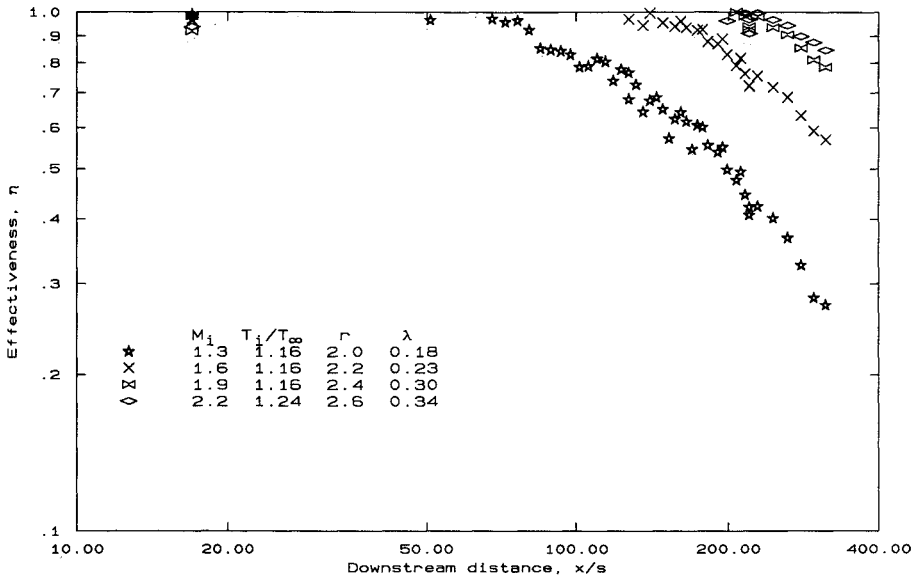

Fig. 8 Heated helium injection, η as a function of x/s.

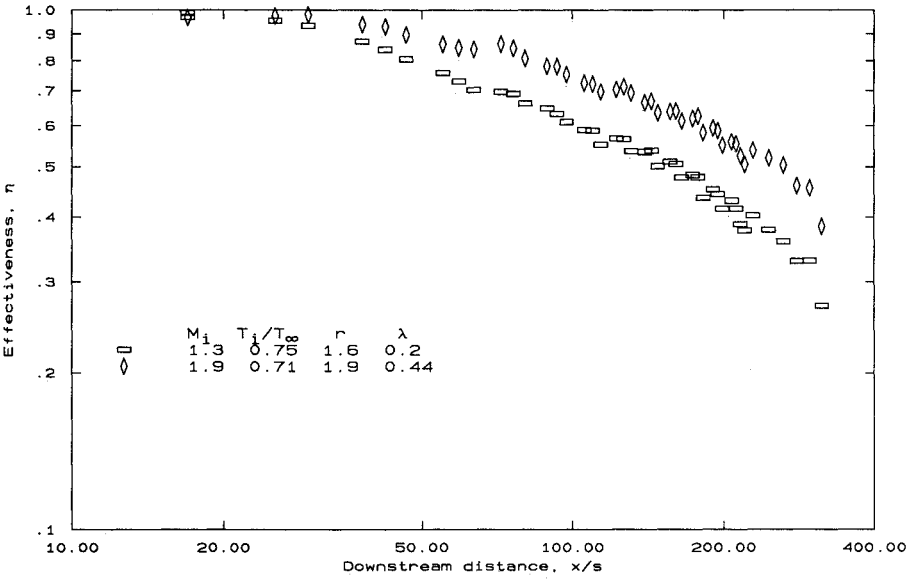

Fig. 9 Cooled helium injection, η as a function of x/s.

the data, with the exception of the cooled helium injection. Figure 10 indicates that the cooling lengths per mass injection rate $X_{cl}/(s\lambda)$ are close for all the air runs, although it appears that the values are slightly larger for the heated air runs. The heated runs also decay at a higher rate than found in the cooled runs, especially for helium. It was shown earlier that there was an initial region where the temperature rose beyond the value at the exit of the slot (apparent in the case of heated injection with $r > 1$). The temperature rise results in higher effectiveness values for heated injection and lower ones for cooled injection. This temperature rise with downstream distance occurs more significantly for helium injection. Therefore, the difference between effectiveness values of the heated and cooled injection is expected to be more significant for helium. In addition to the physical phenomena of increased effectiveness with injectant temperature, higher values of effectiveness for a given $x/(s\lambda)(c_{p\infty}/c_{pi})$ also result from the assumptions made in the integral analysis. The integral analysis that produces the correlation parameter $x/(s\lambda)(c_{p\infty}/c_{pi})$ assumes that the adiabatic wall, $T_{rw}(x)$ in Eq. (2), is equal to the mass averaged temperature downstream of the slot.[8] The mass averaged temperature value is between the adiabatic wall temperature and that of the freestream. Using the adiabatic wall temperature instead of the mass averaged value results in an overestimate of η for heated injection and an underestimate of η for the cooled injection.

In Fig. 10, the experimental results are also compared with the experimental measurements by Goldstein et al.,[11] Cary and Hefner,[12,13] and Rouser and Ewen.[14] To compare these studies, the experimental curves of Cary and Hefner, and of Rouser and Ewen are recalculated from their figures to correspond with the effectiveness definition used in the present work. Also, the curves corresponding to experimental results of Cary and Hefner in Fig. 10 represents bounds of their data. Except for the results of cooled helium injections and that of Rouser and Ewen, the experiments show similar values of the cooling length parameter $X_{cl}/(s\lambda)(c_{p\infty}/c_{pi})$. Beyond $X_{cl}/(s\lambda)(c_{p\infty}/c_{pi})$, the drop in effectiveness is smallest for the hydrogen injection studies by Rouser and Ewen,[14] followed by the results for sonic air injection into a hypersonic freestream by Cary and Hefner.[12,13] The drop in effectiveness of the current experiment is larger than that of Cary and Hefner.[12,13] The difference may be attributed to slower mixing in hypersonic flow boundary layers as compared to the mixing in the current supersonic flow results. The Goldstein et al.[11] results are for a similar Mach number as the present experiments. However,

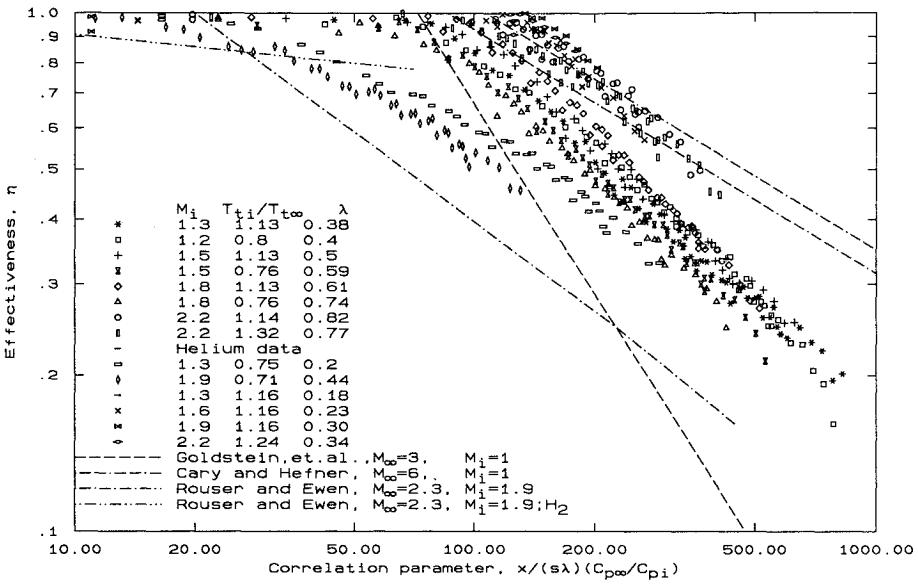

Fig. 10 Comparison of experimental results with previous data using the correlation parameter.

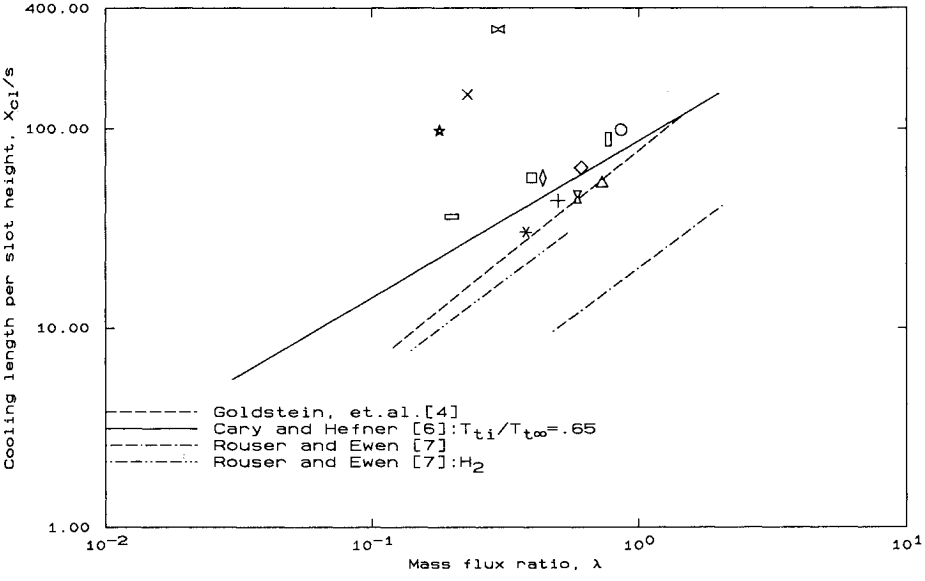

Fig. 11 Symbols correspond to the ones in Fig. 10. X_{cl} as a function of the mass flux ratios.

their results indicate a much steeper decrease in effectiveness which may be due to the relatively large thickness of the nozzle lip as compared to the thickness of the boundary layer. Their geometry may induce a large wake that would enhance mixing between the injectant and the mainstream. The boundary layer to lip thickness ratio of 0.4 in Goldstein's study is small when compared to 6 and 39 of Ref. 25, and 22 and 2.14 of Ref. 19, whose finding was that lip thickness did not affect film cooling. The relatively low air results by Rouser and Ewen[14] are anomalous since the flow conditions are similar to that for the present experiments. Their hydrogen results, as compared with that for air or helium injection, do demonstrate the effect of the increasing the injectant heat capacity.

In several of the references,[4,20,21] other correlation parameters such as $x/(s\lambda^{0.8})$, $x/(s\lambda)Re_i^{-0.25}\nu_\infty/\nu_i$, and $x/(s\lambda)Re_i^{-0.25}(\nu_\infty/\nu_i)(\rho_i/\rho_\infty)^{0.4}[1 + 0.5(\gamma - 1)M_i^2]$ have been used to present the data. These parameters were tried, but the parameters did not indicate a better representation of the results than $x/(s\lambda)(c_{p\infty}/c_{pi})$. Note that these parameters are based on the injection conditions as compared to those of the freestream; as a result these parameters merely shift the curves along the axes of the graph and do not change the slope of the curves.

As a further comparison of the experimental findings, Fig. 11 shows the cooling lengths for each of the experiments as a function of the mass flux ratios. The values of X_{cl} are determined by performing a least squares fit to the data points corresponding to $\eta < 0.80$, and extrapolating the curve to find the $x/(s\lambda)$ value in which $\eta = 1.0$. For the helium injection cases of $M_\infty = 1.9$ and $T_{ti}/T_{t\infty} = 1.16$, only the last point tested is near the value of 0.8, and therefore, the corresponding value of x/s is used. For the case of $M_\infty = 2.2$ and $T_{ti}/T_{t\infty} = 1.24$, all values are larger than 0.8, so its value of X_{cl}/s is not indicated in the figure. For the same injection rate, the helium results show a higher effectiveness than the corresponding air measurements which is due to the relatively high specific heat of helium as compared to that for air. The figure indicates that the heated helium runs clearly have the highest cooling lengths for a given injection rate. The figure shows that the cooling length increases with Mach number for a constant injection rate. The figure also suggests that except for the anomalous cooling run with $M_i = 1.2$, the heating experiments produced larger values of X_{cl}. The cooling lengths for cold helium injection are not significantly larger than the air results; however, as noted earlier the decrease in effectiveness downstream of X_{cl} occurred more slowly. The figure

again indicates the correspondence between the present cooling lengths and the results from Goldstein et al.[11] and Cary and Hefner.[12,13]

Conclusions

The current experiments examine supersonic film cooling effectiveness for air and helium injection. In the experiments, the static pressure between the freestream and the injectant were matched, and the total temperature and Mach number of the injectant were varied. The wall pressure and the wall temperature were measured. The adiabatic wall temperatures were measured directly by insulating the surface.

For heated injection of velocity ratio greater than 1, the temperature increased downstream of the slot, resulting in effectiveness greater than one. This rise is attributed to the deceleration of the injectant as it mixes with the freestream boundary layer and to the transition of the injectant boundary layer.

Generally, effectiveness improves with increasing the injectant Mach number. However, for the cold runs of helium and air, the change in Mach number produces a small change in effectiveness. For λ or r, varying the Mach number of air injection produces a small change in the cooling length per unit mass flux $X_{cl}/(s\lambda)$. In the case of helium injection, keeping λ constant and increasing the Mach number produces a higher cooling length. To vary the injectant Mach number while maintaining the same λ or r, involves changing the temperature. To attribute the increase in cooling length to Mach number alone is not conclusive since the behavior of heated and cooled injection is different. Comparison between helium and air experiments indicates that the effectiveness increases with the heat capacity of the gas.

High effectiveness values far downstream are found with the heated injections for velocity ratios greater than 1. Heated helium injections of velocity ratio greater than 2 produce effectiveness values greater than 0.8 for 300 slot heights downstream of injection point. The increase in temperature downstream of the slot could partly explain the high effectiveness values obtained in the cases of heated injections with $r > 1$.

Previous studies that directly obtained the adiabatic wall temperature are compared with the current experiment. The simple correlation parameter $x/(s\lambda)(c_{p\infty}/c_{pi})$ is demonstrated to be the best choice for correlating the data. However, the cooled helium injection does not conform to this correlation.

Acknowledgments

This work was supported by Caltech's Program in Advanced Technologies, sponsored by Aerojet General, General Motors, and TRW. We would also like to thank Mau Wong for his assistance with the experiments, and E. E. Zukoski for his support.

References

[1]DeMeis, R., "Multimodes to Mach 5," *Aero—Space America*, Vol. 25, No. 9, 1987, pp. 50–53.

[2]Simoneau, R. J., Hendricks, R. C., and Gladden, H. J., "Heat Transfer in Aerospace Propulsion," *Proceedings of ASME National Heat Transfer Conference* (Houston, TX), Vol. 3, 1988, pp. 1–22.

[3]Lucas, J. G., and Golladay, R. L., "Gaseous-Film Cooling of a Rocket Motor with Injection Near the Throat," NASA TN D-3836, Feb. 1967.

[4]Nosek, S. M., and Straight, D. M., "Heat-Transfer Characteristics of Partially Film Cooled Plug Nozzle on A J-85 Afterburning Turbojet Engine," NASA TM X-3362, March 1976.

[5]Gladden, H. J., and Simoneau, R. J., "Review and Assessment of the Database and Numerical Modeling Turbine Heat Transfer," *Symposium Toward Improved Durability in Advanced Aircraft Engine Hot Sections* (Amsterdam, The Netherlands), edited by D. E. Sokolowski, ASME, 1988, pp. 39–56.

[6]Seban, R. A., and Back, L. H. "Velocity and Temperature Profiles in Turbulent Boundary Layer with Tangential Injection," *Journal of Heat Transfer*, Vol. 84, No. 1, 1962, pp. 45–54.

[7]Eckert, E. R. G., and Drake, M. R., Jr., *Analysis of Heat and Mass Transfer*, 2nd ed., McGraw-Hill, New York, 1972, pp. 455–458.

[8]Goldstein, R. J., "Film Cooling," *Advances in Heat Transfer*, Vol. 7, 1971, pp. 321–380.

[9]Beckwith, I. E., and Bushnell, D. M., "Calculation by a Finite-Difference Method of Supersonic Turbulent Boundary Layers with Tangential Slot Injection," NASA TN D-6221, April 1971.

[10]Banken, G. J., Roberts, D. W., Holcomb, J. E., and Birch, S. F., "An Investigation of Film Cooling on a Hypersonic Vehicle Using a P.N.S. Flow Analysis Code," AIAA Paper 85-1591, July 1985.

[11]Goldstein, R. J., Eckert, E. R. G., Tsou, F. K., and Haji-Sheikh, A., "Film Cooling with Air and Helium Injection Through a Rearward-Facing Slot into a Supersonic Air Flow," *AIAA Journal*, Vol. 4, No. 6, 1966, pp. 981–985.

[12]Cary, A. M., and Hefner, J. N., "Film Cooling Effectiveness in Hypersonic Turbulent Flow," *AIAA Journal*, Vol. 8, No. 11, 1970, pp. 2090, 2091.

[13]Cary, A. M., and Hefner, J. N., "Film-Cooling Effectiveness and Skin Friction in Hypersonic Turbulent Flow," *AIAA Journal*, Vol. 10, No. 9, 1972, pp. 1188–1193.

[14]Rousar, D. C., and Ewen, R. L., "Hydrogen Film Cooling Investigation," NASA CR 121235, Aug. 1973.

[15]Baryshev, Y. V., Leont'yev, A. I., and Rozhdestvenskiy, V. I., "Heat Transfer in the Zone of Interaction Between a Shock and the Boundary Layer," *Heat Transfer—Soviet Research*, Vol. 7, No. 6, 1975, pp. 19–23.

[16]Alzner, E., and Zakkay, V., "Turbulent Boundary Layer Shock Interaction with and Without Injection," *AIAA Journal*, Vol. 9, No. 9, 1971, pp. 1769–1776.

[17]Zakkay, V., Sakell, L., and Parthasarathy, K., "An Experimental Investigation of Supersonic Slot Cooling," *Proceedings of the 1970 Heat Transfer and Fluid Mechanics Institute*, edited by T. Sarpkaya, Stanford Univ. Press, Stanford, CA, 1970, pp. 88–103.

[18]Parthasarathy, K., and Zakkay, V., "An Experimental Investigation of Turbulent Slot Injection at Mach 6," *AIAA Journal*, Vol. 8, No. 7, 1970, pp. 1302–1307.

[19]Olsen, G. C., Nowak, R. J., Holden, M. S., and Baker, N. R., "Experimental Results for Film Cooling in 2-D Supersonic Flow Including Coolant Delivery Pressure, Geometry and Incident Shock Effects," AIAA Paper 90-0605, Jan. 1990.

[20]Holden, M. S., Nowak, R. J., Olsen, G. C., and Rodriguez, K. M., "Experimental Studies of Shock Wave/Wall Jet Interaction in Hypersonic Flow," AIAA Paper 90-0607, Jan. 1990.

[21]Majeski, J. A., and Weatherford, R. H., "Development of an Empirical Correlation for Film-Cooling Effectiveness," AIAA Paper 88-2624, June 1988.

[22]Juhany, K. A., and Hunt, M. L., "Flow-Field Measurements in Supersonic Film Cooling Including the Effect of Shock Wave Interaction," *AIAA Journal* (submitted for publication).

[23]Juhany, K. A., "Supersonic Film Cooling Including the Effect of Shock Wave Interaction," Ph.D. Dissertation, California Inst. of Technology, Pasadena, CA, 1993.

[24]Lappas, A., "An Adaptive Lagrangian Method for Computing 1-D Reacting Flows and the Theory of Riemann Invariant Manifolds for the Compressible Euler Equations," Ph.D. Dissertation, California Inst. of Technology, Pasadena, CA, 1993.

[25]Hefner, J. N., "Effect of Geometry Modification on Effectiveness of Slot Injection in Hypersonic Flow," *AIAA Journal*, Vol. 14, No. 6, 1976, pp. 817, 818.